

Measurement of the branching fractions for $B^0 \rightarrow D_s^{*+} \pi^-$ and $B^0 \rightarrow D_s^{*-} K^+$ decays

N. J. Joshi,³⁹ T. Aziz,³⁹ K. Trabelsi,⁸ I. Adachi,⁸ H. Aihara,⁴³ K. Arinstein,^{1,32} V. Aulchenko,^{1,32} T. Aushev,^{18,12}
 A. M. Bakich,³⁸ V. Balagura,¹² E. Barberio,²² A. Bay,¹⁸ K. Belous,¹¹ V. Bhardwaj,³⁴ M. Bischofberger,²⁴
 A. Bondar,^{1,32} A. Bozek,²⁸ M. Bračko,^{20,13} T. E. Browder,⁷ M.-C. Chang,⁴ P. Chang,²⁷ Y. Chao,²⁷ A. Chen,²⁵
 P. Chen,²⁷ B. G. Cheon,⁶ I.-S. Cho,⁴⁷ Y. Choi,³⁷ J. Dalseno,^{21,40} A. Das,³⁹ Z. Doležal,² Z. Drásal,² A. Drutskoy,³
 S. Eidelman,^{1,32} N. Gabyshev,^{1,32} P. Goldenzweig,³ B. Golob,^{19,13} H. Ha,¹⁶ J. Haba,⁸ B.-Y. Han,¹⁶ K. Hayasaka,²³
 H. Hayashii,²⁴ M. Hazumi,⁸ Y. Horii,⁴² Y. Hoshi,⁴¹ W.-S. Hou,²⁷ Y. B. Hsiung,²⁷ H. J. Hyun,¹⁷ T. Iijima,²³
 K. Inami,²³ R. Itoh,⁸ M. Iwabuchi,⁴⁷ M. Iwasaki,⁴³ Y. Iwasaki,⁸ T. Julius,²² J. H. Kang,⁴⁷ T. Kawasaki,³⁰
 H. J. Kim,¹⁷ H. O. Kim,¹⁷ J. H. Kim,³⁷ S. K. Kim,³⁶ Y. I. Kim,¹⁷ Y. J. Kim,⁵ K. Kinoshita,³ B. R. Ko,¹⁶
 P. Kodyš,² M. Kreps,¹⁵ P. Križan,^{19,13} P. Krokovny,⁸ T. Kuhr,¹⁵ A. Kuzmin,^{1,32} Y.-J. Kwon,⁴⁷ S.-H. Kyeong,⁴⁷
 M. J. Lee,³⁶ S.-H. Lee,¹⁶ J. Li,⁷ C. Liu,³⁵ Y. Liu,²³ D. Liventsev,¹² R. Louvot,¹⁸ A. Matyja,²⁸ S. McOnie,³⁸
 K. Miyabayashi,²⁴ Y. Miyazaki,²³ R. Mizuk,¹² T. Mori,²³ E. Nakano,³³ M. Nakao,⁸ Z. Natkaniec,²⁸ S. Neubauer,¹⁵
 S. Nishida,⁸ K. Nishimura,⁷ O. Nitoh,⁴⁵ S. Ogawa,⁴⁸ T. Ohshima,²³ S. Okuno,¹⁴ S. L. Olsen,^{36,7} G. Pakhlova,¹²
 C. W. Park,³⁷ H. Park,¹⁷ H. K. Park,¹⁷ M. Petrič,¹³ L. E. Piiilonen,⁴⁶ A. Poluektov,^{1,32} S. Ryu,³⁶ H. Sahoo,⁷
 K. Sakai,³⁰ Y. Sakai,⁸ O. Schneider,¹⁸ C. Schwanda,¹⁰ A. J. Schwartz,³ K. Senyo,²³ M. E. Sevior,²² M. Shapkin,¹¹
 C. P. Shen,⁷ J.-G. Shiu,²⁷ B. Shwartz,^{1,32} J. B. Singh,³⁴ P. Smerkol,¹³ A. Sokolov,¹¹ E. Solovieva,¹²
 S. Stanič,³¹ M. Starič,¹³ J. Stypula,²⁸ T. Sumiyoshi,⁴⁴ G. N. Taylor,²² Y. Teramoto,³³ S. Uehara,⁸ Y. Unno,⁶
 S. Uno,⁸ Y. Usov,^{1,32} G. Varner,⁷ K. E. Varvell,³⁸ K. Vervink,¹⁸ C. H. Wang,²⁶ M.-Z. Wang,²⁷ P. Wang,⁹
 X. L. Wang,⁹ Y. Watanabe,¹⁴ R. Wedd,²² J. Wiechczynski,²⁸ E. Won,¹⁶ B. D. Yabsley,³⁸ Y. Yamashita,²⁹
 M. Yamauchi,⁸ C. C. Zhang,⁹ Z. P. Zhang,³⁵ V. Zhilich,^{1,32} T. Zivko,¹³ A. Zupanc,¹³ and O. Zyukova^{1,32}

(The Belle Collaboration)

¹*Budker Institute of Nuclear Physics, Novosibirsk*

²*Faculty of Mathematics and Physics, Charles University, Prague*

³*University of Cincinnati, Cincinnati, Ohio 45221*

⁴*Department of Physics, Fu Jen Catholic University, Taipei*

⁵*The Graduate University for Advanced Studies, Hayama*

⁶*Hanyang University, Seoul*

⁷*University of Hawaii, Honolulu, Hawaii 96822*

⁸*High Energy Accelerator Research Organization (KEK), Tsukuba*

⁹*Institute of High Energy Physics, Chinese Academy of Sciences, Beijing*

¹⁰*Institute of High Energy Physics, Vienna*

¹¹*Institute of High Energy Physics, Protvino*

¹²*Institute for Theoretical and Experimental Physics, Moscow*

¹³*J. Stefan Institute, Ljubljana*

¹⁴*Kanagawa University, Yokohama*

¹⁵*Institut für Experimentelle Kernphysik, Karlsruhe Institut für Technologie, Karlsruhe*

¹⁶*Korea University, Seoul*

¹⁷*Kyungpook National University, Taegu*

¹⁸*École Polytechnique Fédérale de Lausanne (EPFL), Lausanne*

¹⁹*Faculty of Mathematics and Physics, University of Ljubljana, Ljubljana*

²⁰*University of Maribor, Maribor*

²¹*Max-Planck-Institut für Physik, München*

²²*University of Melbourne, School of Physics, Victoria 3010*

²³*Nagoya University, Nagoya*

²⁴*Nara Women's University, Nara*

²⁵*National Central University, Chung-li*

²⁶*National United University, Miao Li*

²⁷*Department of Physics, National Taiwan University, Taipei*

²⁸*H. Niewodniczanski Institute of Nuclear Physics, Krakow*

²⁹*Nippon Dental University, Niigata*

arXiv:0912.2594v2 [hep-ex] 23 Jan 2010

- ³⁰*Niigata University, Niigata*
³¹*University of Nova Gorica, Nova Gorica*
³²*Novosibirsk State University, Novosibirsk*
³³*Osaka City University, Osaka*
³⁴*Panjab University, Chandigarh*
³⁵*University of Science and Technology of China, Hefei*
³⁶*Seoul National University, Seoul*
³⁷*Sungkyunkwan University, Suwon*
³⁸*School of Physics, University of Sydney, NSW 2006*
³⁹*Tata Institute of Fundamental Research, Mumbai*
⁴⁰*Excellence Cluster Universe, Technische Universität München, Garching*
⁴¹*Tohoku Gakuin University, Tagajo*
⁴²*Tohoku University, Sendai*
⁴³*Department of Physics, University of Tokyo, Tokyo*
⁴⁴*Tokyo Metropolitan University, Tokyo*
⁴⁵*Tokyo University of Agriculture and Technology, Tokyo*
⁴⁶*IPNAS, Virginia Polytechnic Institute and State University, Blacksburg, Virginia 24061*
⁴⁷*Yonsei University, Seoul*
⁴⁸*Toho University, Funabashi*

Abstract

We present a study of $B^0 \rightarrow D_s^{*+}\pi^-$ and $B^0 \rightarrow D_s^{*-}K^+$ decays based on a sample of 657×10^6 $B\bar{B}$ events collected with the Belle detector at the KEKB asymmetric-energy e^+e^- collider. We measure the branching fractions to be $\mathcal{B}(B^0 \rightarrow D_s^{*+}\pi^-) = (1.75 \pm 0.34 \text{ (stat)} \pm 0.17 \text{ (syst)} \pm 0.11 \text{ (}\mathcal{B}\text{)}) \times 10^{-5}$ and $\mathcal{B}(B^0 \rightarrow D_s^{*-}K^+) = (2.02 \pm 0.33 \text{ (stat)} \pm 0.18 \text{ (syst)} \pm 0.13 \text{ (}\mathcal{B}\text{)}) \times 10^{-5}$, with significances of 6.1 and 8.0 standard deviations, respectively. The first uncertainty is statistical, the second is due to the experimental systematics, and the third is from uncertainties in the D_s^+ decay branching fractions. From our measurements, we obtain the most precise determination so far of $R_{D^*\pi}$, where $R_{D^*\pi}$ is the ratio between amplitudes of the doubly Cabibbo-suppressed decay $B^0 \rightarrow D^{*+}\pi^-$ and the Cabibbo favored $B^0 \rightarrow D^{*-}\pi^+$ decay.

PACS numbers: 11.30.Er, 12.15.Hh, 13.25.Hw

In the standard model (SM), CP violation arises naturally when the Cabibbo-Kobayashi-Maskawa (CKM) mixing matrix is introduced into the weak-interaction Lagrangian [1]. A precise measurement of the CKM parameters is crucial for understanding CP violation in the SM. In particular, the time-dependent CP analysis of the $B^0(\bar{B}^0) \rightarrow D^{*\mp}\pi^\pm$ system provides a theoretically clean measurement of the product $R_{D^*\pi} \sin(2\phi_1 + \phi_3)$ [2], where ϕ_1 and ϕ_3 are interior angles of the unitarity triangle and $R_{D^*\pi}$ is the ratio of the magnitudes of the doubly Cabibbo-suppressed decay (DCSD) amplitude (Fig. 1(b)) to the Cabibbo-favored decay (CFD) amplitude (Fig. 1(a)). Measuring the DCSD amplitude is not possible with the current data, due to the overwhelming background from $\bar{B}^0 \rightarrow D^{*+}\pi^-$ and hence, it is not possible to extract the angle ϕ_3 from this study alone unless an independent measurement of $R_{D^*\pi}$ is provided externally. The mode $B^+ \rightarrow D^{*+}\pi^0$ may be used to estimate the size of DCSD, since $B^0 \rightarrow D^{*+}\pi^-$ and $B^+ \rightarrow D^{*+}\pi^0$ are related by isospin symmetry [2]. However, the $B^+ \rightarrow D^{*+}\pi^0$ branching fraction is small and so far only an upper limit has been obtained [3]. Unlike the $B^0 \rightarrow D^{*\mp}\pi^\pm$ system, $B^0 \rightarrow D_s^{*+}\pi^-$, which is predominantly a spectator process with a $b \rightarrow u$ transition (Fig. 1(c)), does not have contributions from \bar{B}^0 decays to the same final state and can provide clean experimental access to $R_{D^*\pi}$. Assuming SU(3) flavor symmetry

between D^* and D_s^* , $R_{D^*\pi}$ is given by

$$R_{D^*\pi} = \tan \theta_C \left(\frac{f_{D^*}}{f_{D_s^*}} \right) \sqrt{\frac{\mathcal{B}(B^0 \rightarrow D_s^{*+}\pi^-)}{\mathcal{B}(B^0 \rightarrow D^{*-}\pi^+)}} \quad (1)$$

where θ_C is the Cabibbo angle, f_{D^*} and $f_{D_s^*}$ are the meson form factors, and the \mathcal{B} 's stand for the corresponding branching fractions. The $B^0 \rightarrow D_s^{*+}\pi^-$ process, in addition, does not have a penguin loop contribution and hence can in principle be used to determine $|V_{ub}|$ [4].

In contrast to the $B^0 \rightarrow D^{*\mp}\pi^\pm$ decays shown in Figs. 1(d) and (e), the $B^0 \rightarrow D_s^{*+}\pi^-$ decay does not have a contribution from the W -exchange amplitude, as the quark-antiquark pair with the same flavor, required for such a diagram, is absent from the final state. We assume the W -exchange contributions in $B^0 \rightarrow D^{*\mp}\pi^\pm$ to be negligible, in making the correspondence between $D^{*+}\pi^-$ and $D_s^{*+}\pi^-$ in the $R_{D^*\pi}$ calculation. The size of the W -exchange diagram can be estimated from the $B^0 \rightarrow D_s^{*-}K^+$ decay, which proceeds only via W -exchange (Fig. 1(f)). The $B^0 \rightarrow D_s^{*-}K^+$ branching fraction was expected to be enhanced due to rescattering effects [5]. However, a recent theoretical study based on measurements of related processes indicates the absence of such an enhancement [6].

While $B^0 \rightarrow D_s^+\pi^-$ and $B^0 \rightarrow D_s^-K^+$ decays have been observed previously by Belle [7] and BaBar [8], the observations of the modes $B^0 \rightarrow D_s^{*+}\pi^-$ and $B^0 \rightarrow$

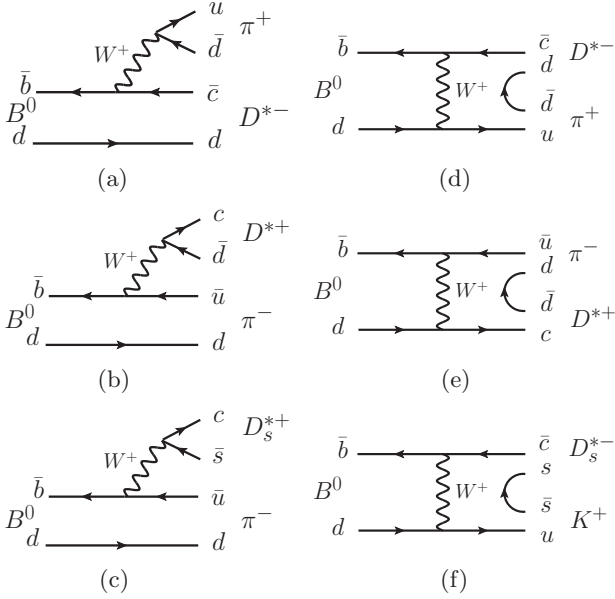


FIG. 1: Feynman diagrams for (a) Cabibbo-favored decay $B^0 \rightarrow D^{*-}\pi^+$, (b) doubly Cabibbo-suppressed decay $B^0 \rightarrow D_s^{*+}\pi^-$, (c) SU(3) flavor symmetric $B^0 \rightarrow D_s^{*+}\pi^-$; color suppressed W -exchange contributions (d) to $B^0 \rightarrow D^{*-}\pi^+$, (e) to $B^0 \rightarrow D_s^{*+}\pi^-$ and (f) to the decay $B^0 \rightarrow D_s^{*-}K^+$.

$D_s^{*-}K^+$ have been reported by BaBar [9, 10], which measured $\mathcal{B}(B^0 \rightarrow D_s^{*+}\pi^-) = (2.6_{-0.4}^{+0.5} \pm 0.3) \times 10^{-5}$ and $\mathcal{B}(B^0 \rightarrow D_s^{*-}K^+) = (2.4 \pm 0.4 \pm 0.2) \times 10^{-5}$. In this paper, we report an improved measurement of the branching fractions for the decays $B^0 \rightarrow D_s^{*+}\pi^-$ and $B^0 \rightarrow D_s^{*-}K^+$ [11] with a data sample consisting of $657 \times 10^6 B\bar{B}$ pairs, collected with the Belle detector at the KEKB asymmetric-energy e^+e^- collider [12].

The Belle detector is a large-solid-angle magnetic spectrometer that consists of a silicon vertex detector, a 50-layer central drift chamber (CDC), an array of aerogel threshold Cherenkov counters (ACC), a barrel-like arrangement of time-of-flight scintillation counters (TOF), and an electromagnetic calorimeter comprised of CsI(Tl) crystals located inside a superconducting solenoid coil that provides a 1.5 T magnetic field. An iron flux-return yoke located outside the solenoid is instrumented to detect K_L^0 mesons and to identify muons. The detector is described in detail elsewhere [13]. Two different inner detector configurations were used. For the first sample of $152 \times 10^6 B\bar{B}$ pairs, a 2.0 cm radius beam-pipe and a 3-layer silicon vertex detector were used; for the latter $505 \times 10^6 B\bar{B}$ pairs, a 1.5 cm radius beam-pipe with a 4-layer silicon vertex detector and a small-cell inner drift chamber were used [14].

The signal is reconstructed in three D_s^+ modes: $\phi\pi^+$ with $\phi \rightarrow K^+K^-$, $\bar{K}^*(892)^0K^+$ with $\bar{K}^*(892)^0 \rightarrow K^-\pi^+$, and $K_S^0K^+$ with $K_S^0 \rightarrow \pi^+\pi^-$. Charged tracks are selected with requirements based on the impact parameter relative to the interaction point (IP). The deviations from the IP are required to be within ± 4 cm along

the z -axis (the direction opposite to the positron beam) and within 0.2 cm in the $x-y$ plane. We also require the transverse momentum of the tracks to be greater than 0.1 GeV/c in order to reduce low momentum combinatorial background.

For charged particle identification (PID), we combine the information from the specific ionization (dE/dx) in the CDC with measurements from the TOF and ACC. At large momenta ($p > 2.5$ GeV/c) only the ACC measurement and dE/dx are used. We assign likelihood values \mathcal{L}_K (\mathcal{L}_π) for the kaon (pion) hypothesis to each charged track. Tracks are identified based on the ratio $\mathcal{R}_{K/\pi} = \mathcal{L}_K/(\mathcal{L}_K + \mathcal{L}_\pi)$, which peaks at one for real kaons and at zero for real pions. For the prompt kaon (pion) track, we require $\mathcal{R}_{K/\pi} > 0.6$ (< 0.6), for which the identification efficiency is 85% (92%) with a pion (kaon) fake-rate of 8% (15%). Due to the low background level for modes with a ϕ meson, less restrictive PID cuts of $\mathcal{R}_{K/\pi} > 0.2$ are applied to the ϕ daughter tracks.

The ϕ ($\bar{K}^*(892)^0$) mesons are required to have an invariant mass within ± 14 MeV/ c^2 (± 75 MeV/ c^2) of the nominal ϕ ($\bar{K}^*(892)^0$) mass [15]. We reconstruct K_S^0 candidates from $\pi^+\pi^-$ pairs, requiring the invariant mass to be within ± 10 MeV/ c^2 ($\sim \pm 3\sigma$) of the nominal K_S^0 mass. The K_S^0 candidate is further required to pass a momentum-dependent selection criteria based on its vertex topology, the flight length in the $r-\phi$ plane, and the daughter π^\pm momentum distribution [16]. The D_s^+ candidate mass window for $\phi\pi^+$, $\bar{K}^*(892)^0K^+$, and $K_S^0K^+$ modes is ± 13 MeV/ c^2 , ± 15 MeV/ c^2 , and ± 17 MeV/ c^2 , respectively; these ranges correspond to approximately 3σ in resolution around the D_s^+ mass. To reduce combinatorial background, we use a more stringent PID requirement for the kaon accompanying the $\bar{K}^*(892)^0$, $\mathcal{R}_{K/\pi} > 0.8$. The D_s^+ candidate is constrained kinematically to have a mass equal to the nominal value [15].

The D_s^{*+} mesons are reconstructed by combining the D_s^+ candidates with a photon. The photons are reconstructed from energy depositions in the ECL and are required to have energies greater than 60 MeV (100 MeV) in the barrel (endcap) region covering the polar angle $32^\circ < \theta < 128^\circ$ ($17^\circ < \theta < 32^\circ$ (forward endcap) and $128^\circ < \theta < 150^\circ$ (backward endcap)). The D_s^{*+} candidate is required to have $\Delta M = M_{D_s^+\gamma} - M_{D_s^+}$ between 128 MeV/ c^2 and 162 MeV/ c^2 , where $M_{D_s^+\gamma}$ and $M_{D_s^+}$ are the invariant masses of the $D_s^+\gamma$ system and the D_s^+ candidate, respectively. To reduce the combinatorial background due to low energy photons, we require that $\cos\theta_{D_s^{*+}} > -0.6$ (-0.7) for $B^0 \rightarrow D_s^{*+}\pi^-$ ($B^0 \rightarrow D_s^{*+}K^+$), where $\theta_{D_s^{*+}}$ is defined as the angle between the flight direction of the photon and the direction opposite to the B^0 flight in the D_s^{*+} rest frame. We then perform a mass-constrained fit to the D_s^{*+} candidate. This improves the momentum resolution by 25%.

The B^0 candidates, reconstructed by combining a D_s^{*+} candidate with an oppositely charged pion/kaon track, are identified by the energy difference, $\Delta E = \sum_i E_i -$

E_{beam} and the beam-energy constrained mass, $M_{\text{bc}} = \sqrt{E_{\text{beam}}^2 - (\sum_i \vec{p}_i)^2}$, where E_{beam} is the beam energy in the $\Upsilon(4S)$ center-of-mass (CM) frame and \vec{p}_i and E_i are the momentum and energy of the i th daughter of the B^0 in the CM frame. We retain B^0 candidates with ΔE within ± 0.2 GeV and M_{bc} between $5.2 \text{ GeV}/c^2$ and $5.3 \text{ GeV}/c^2$ for further analysis.

The dominant background comes from the $e^+e^- \rightarrow q\bar{q}$ ($q = u, d, s$ and c quarks) continuum process. To suppress this background, we use the event topology in the CM frame to distinguish more spherical $B\bar{B}$ events from the jet-like continuum events. A likelihood function $\mathcal{R} = \mathcal{L}_{\text{sig}}/(\mathcal{L}_{\text{sig}} + \mathcal{L}_{\text{bkg}})$ is prepared by combining a Fisher discriminant, based on a set of modified Fox-Wolfram moments [17, 18] with $\cos\theta_B$, where θ_B is the polar angle of the B^0 meson flight direction in the CM frame. The angle θ_B follows a $\sin^2\theta_B$ distribution for $B\bar{B}$ events, while the continuum distribution is flat. The selection criteria for \mathcal{R} are determined by maximizing a figure-of-merit, $S/\sqrt{S+B}$, where S and B are the number of signal and background events determined from large Monte Carlo (MC) samples [19], with statistics corresponding to about 100 (5) times data for signal (background) MC. The signal yield, S is obtained assuming the latest branching fraction measurements [15]. In the case of $B^0 \rightarrow D_s^{*+}\pi^-$ ($B^0 \rightarrow D_s^{*-}K^+$), we require \mathcal{R} to be greater than 0.45 (0.45) for the $\phi\pi$ mode, 0.50 (0.60) for the $\bar{K}^*(892)^0K$ mode, and 0.40 (0.40) for the K_S^0K mode. For the $\phi\pi$ mode, this requirement suppresses 80% of the continuum background, while retaining 85% of the signal.

About 15% of events have more than one B^0 signal candidate. For these events we choose the candidate with the M_{bc} value closest to the nominal B^0 mass. This procedure selects the correct B^0 candidate in about 92% of the cases. Only events with M_{bc} between $5.27 \text{ GeV}/c^2$ and $5.29 \text{ GeV}/c^2$ are considered for further analysis, while the signal is extracted by performing a fit to the ΔE distribution. We define the fit region to be $|\Delta E| < 0.2$ GeV.

A MC sample of $B\bar{B}$ events is used to determine possible backgrounds that can enter the ΔE fit region. In both signal modes ($B^0 \rightarrow D_s^*h$, where h is a charged K or π), about 45% of the background comes from decays involving a $D^+ \rightarrow K^-\pi^+\pi^+$ or a $D^+ \rightarrow K_S^0\pi^+$ sub-decay, which form a fake D_s^+ when the π^+ from the D^+ is misidentified as a K^+ . However, these events do not peak and are distributed over the entire fit region due to the addition of a random photon.

On the other hand, some rare B decays to final states that contain a correctly reconstructed $D_s^{(*)+}$ produce non-negligible peaking structures in the ΔE fit region: $B^0 \rightarrow D_s^+\pi^-$ ($B^0 \rightarrow D_s^-K^+$) events populate the region around 150 MeV due to the addition of an extra photon, $B^0 \rightarrow D_s^{*+}\rho^-$ ($B^+ \rightarrow D_s^{*-}K^+\pi^+$) events populate the region around -150 MeV, since a π^0 (π^+) is not reconstructed, while the events from $B^0 \rightarrow D_s^+\rho^-$ ($B^+ \rightarrow D_s^-K^+\pi^+$) are distributed around -50 MeV,

with the extra photon compensating the lost pion. These backgrounds are represented by PDFs with fixed yields. MC samples are used to determine the PDF parameters as well as efficiencies. The yields are calculated assuming the most recent known values for their branching fractions [10, 15]. Apart from the backgrounds discussed above, the two B^0 signal modes cross-feed each other. We use signal MCs to determine the PDFs for the cross-feeds. ΔM sidebands in the data are used to verify the consistency of the MC background predictions with the data.

The signal PDF is the sum of a Crystal Ball line-shape [20] and a broad Gaussian and is parametrized using signal MC samples generated in each D_s^+ mode. The signal as well as the peaking background PDFs are subsequently corrected for possible differences in the parameter values between MC and real data, using a $B^0 \rightarrow D_s^{*+}D^-$ data control sample. The combinatorial backgrounds in each mode are accounted for by adding linear functions.

We determine the branching fractions from a simultaneous unbinned extended maximum likelihood fit to the ΔE distributions of the three D_s^+ decay modes for each signal mode. To account for the cross-feeds between the signal modes due to the misidentification of the prompt track, the two B signal modes are fitted simultaneously, with the $B^0 \rightarrow D_s^{*-}K^+$ signal yield in the correctly reconstructed sample determining the normalization of the cross-feed in the $B^0 \rightarrow D_s^{*+}\pi^-$ fit region, and vice versa. The fit has 14 free parameters: the branching fractions of the signal modes (2), and the yields and slopes of the first-order polynomials representing the combinatorial background in each of the three D_s^+ modes (12). Figure 2 shows results of the simultaneous fit for the three D_s^+ modes in both signal modes. We summarize the results of the fits in Table I. The significance is defined as $\sqrt{-2\ln(\mathcal{L}_0/\mathcal{L}_{\text{max}})}$, where \mathcal{L}_{max} (\mathcal{L}_0) are the likelihoods for the best fit and with the signal branching fraction fixed to zero.

The major source of systematic uncertainty in the branching fraction measurement of $B^0 \rightarrow D_s^{*+}\pi^-$ ($B^0 \rightarrow D_s^{*-}K^+$) is the uncertainty in the branching fractions of the D_s^+ decays, which amount to 5.9% (6.2%). The uncertainties in the branching fractions of the peaking background modes contribute an additional error of 1.5% (1.9%). The systematic uncertainty in the tracking efficiency is estimated to be about 1.0% per track. The uncertainty in the PID efficiency is about 2.4% (2.1%). Photon detection efficiency has an uncertainty of 7.0%, while K_S^0 detection efficiency adds 1.1% uncertainty in the result. The efficiency of the \mathcal{R} requirement, used to suppress the continuum background, introduces an uncertainty of 0.6% (0.5%) in the branching fraction. The limited size of the MC samples used to determine efficiencies and cross-feed fractions introduces an error of 1.4% (1.6%). The uncertainty in the determination of the signal PDF shape is about 3.4% (1.5%). Estimation of possible bias in the fit results in another 0.9% (0.3%)

TABLE I: Efficiency (ϵ), yield (N_{sig}), branching fraction (\mathcal{B}) and statistical significance not including systematic errors (\mathcal{S}) from the fits to the data obtained individually in the three D_s^+ modes as well as from the simultaneous fit. The second error on the \mathcal{B} 's is due to the uncertainties in D_s^+ decay branching fractions. The individual fit results are consistent with each other and also with the simultaneous fit. Note that the efficiencies in the $K_S^0 K$ mode include the $K_S^0 \rightarrow \pi^+ \pi^-$ decay branching fraction.

B^0 mode	D_s^+ mode	ϵ (%)	N_{sig}	$\mathcal{B}(10^{-5})$	$\mathcal{S} (\sigma)$
$B^0 \rightarrow D_s^{*+} \pi^-$	$\phi(K^+ K^-) \pi^+$	15.2	32 ± 8	$1.58 \pm 0.40 \pm 0.24$	3.2
	$\bar{K}^*(892)^0(K^- \pi^+) K^+$	7.9	29 ± 10	$2.30 \pm 0.76 \pm 0.35$	2.6
	$K_S^0 K^+$	8.0	13 ± 7	$1.78 \pm 0.92 \pm 0.11$	2.2
	Simultaneous	-	-	$1.75 \pm 0.34 \pm 0.11$	6.6
$B^0 \rightarrow D_s^{*-} K^+$	$\phi(K^+ K^-) \pi^+$	13.4	33 ± 8	$1.81 \pm 0.41 \pm 0.27$	3.2
	$\bar{K}^*(892)^0(K^- \pi^+) K^+$	6.4	23 ± 7	$2.22 \pm 0.66 \pm 0.34$	2.8
	$K_S^0 K^+$	6.9	14 ± 5	$2.14 \pm 0.80 \pm 0.13$	3.1
	Simultaneous	-	-	$2.02 \pm 0.33 \pm 0.13$	8.6

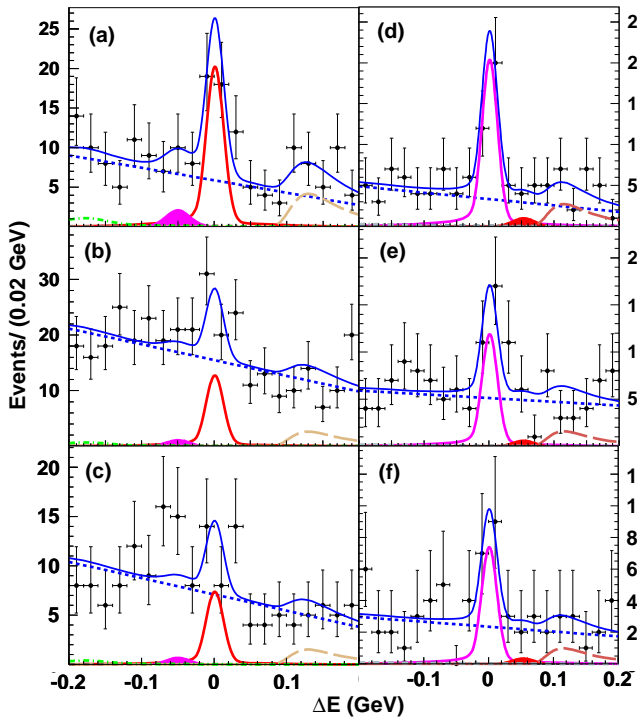


FIG. 2: The simultaneous fit in the $B^0 \rightarrow D_s^{*+} \pi^-$ ((a) $\phi\pi$, (b) $\bar{K}^* K$ and (c) $K_S^0 K$ mode) and the $B^0 \rightarrow D_s^{*-} K^+$ ((d)-(f)) signal modes. Signal peaks are shown by the solid curves while the solid-filled curves represent the cross-feed contributions from the other B^0 signal modes. The long-dashed curves correspond to the contribution from the $B \rightarrow D_s \pi$ ($B \rightarrow D_s K$) and the dot-dashed curves to that from $B^0 \rightarrow D_s^{(*)+} \rho^-$ ($B^+ \rightarrow D_s^{(*)-} K^+ \pi^+$). The dotted curves correspond to the combinatorial background.

uncertainty.

Table II summarizes the systematic uncertainties involved. The overall systematic error is obtained by adding the above contributions in quadrature.

We obtain $\mathcal{B}(B^0 \rightarrow D_s^{*+} \pi^-) = (1.75 \pm 0.34 \text{ (stat)} \pm$

TABLE II: Contributions to the systematic uncertainty

Source	Contribution(%)	
	$D_s^{*+} \pi^-$	$D_s^{*-} K^-$
D_s^+ branching fraction uncertainties		
signal	5.9	6.2
peaking background	1.5	1.9
Total (\mathcal{B})	6.1	6.5
Tracking efficiency	4.0	4.0
Photon detection efficiency	7.0	7.0
Particle identification efficiency	2.4	2.1
K_S^0 efficiency	1.1	1.1
\mathcal{LR}	0.6	0.5
$N_{B\bar{B}}$	1.4	1.4
MC statistics	1.4	1.6
PDF shape	3.4	1.5
Fit bias	0.9	0.3
Total (other)	9.4	8.8

$0.17 \text{ (syst)} \pm 0.11 \text{ (}\mathcal{B}\text{)} \times 10^{-5}$ and $\mathcal{B}(B^0 \rightarrow D_s^{*-} K^+) = (2.02 \pm 0.33 \text{ (stat)} \pm 0.18 \text{ (syst)} \pm 0.13 \text{ (}\mathcal{B}\text{)}) \times 10^{-5}$ with significances of 6.1σ and 8.0σ , respectively, where the systematic uncertainties on the signal yield as well as the statistical uncertainties are included in the significance evaluation. Though consistent with the previous measurements [10], we observe slightly lower branching fractions. Using the observed value for the $B^0 \rightarrow D_s^{*+} \pi^-$ branching fraction, the latest values for $\mathcal{B}(B^0 \rightarrow D_s^{*-} \pi^+) = (2.76 \pm 0.13) \times 10^{-3}$, $\tan\theta_C = 0.2314 \pm 0.0021$ [15], and the theoretical estimate of the ratio $f_{D_s^+}/f_{D^+} = (1.164 \pm 0.006 \text{ (stat)} \pm 0.020 \text{ (syst)})$ [21], we obtain,

$$R_{D^* \pi} = (1.58 \pm 0.15 \text{ (stat)} \pm 0.10 \text{ (syst)} \pm 0.03 \text{ (th)})\%,$$

where the first error is statistical, the second corresponds to the experimental systematic uncertainty and the third accounts for the theoretical uncertainty in the $f_{D_s^+}/f_{D^+}$

estimation. We have assumed that the ratio f_{D_s}/f_D is equal to the ratio of vector meson decay constants, $f_{D_s^*}/f_{D^*}$. The quenched QCD approximation [22] as well as the heavy quark effective theory predictions [23] point toward an uncertainty of about 1% due to this assumption, which is included in our estimation of $R_{D^*\pi}$. The value we obtain for $R_{D^*\pi}$, though consistent with the theoretical expectation of 2%, is slightly smaller than the previous estimate [10].

The observed value for the $B^0 \rightarrow D_s^{*-} K^+$ branching fraction is two orders of magnitude lower than that for the Cabibbo-favored decay $B^0 \rightarrow D^{*-} \pi^+$. This can be understood purely in terms of the exchange amplitude and there is no evidence for enhancement due to rescattering effects, which would lead to comparable amplitudes for the two processes [5]. From this same comparison, we find no evidence for large W -exchange contributions to $B^0 \rightarrow D^{*\mp} \pi^\pm$; such contributions are assumed to be small, in the determination of $R_{D^*\pi}$ (Eq. 1).

In conclusion, we report the most precise measurement of the $B^0 \rightarrow D_s^{*+} \pi^-$ and $B^0 \rightarrow D_s^{*-} K^+$ decay branching fractions. This improves the precision with which the parameter $R_{D^*\pi}$ can be estimated, and thus the prospect of determining ϕ_3 from measurements of CP violating effects in the $D^{*\pm} \pi^\mp$ system.

We thank the KEKB group for the excellent operation of the accelerator, the KEK cryogenics group for the efficient operation of the solenoid, and the KEK computer group and the National Institute of Informatics for valuable computing and SINET3 network support.

We acknowledge support from the Ministry of Education, Culture, Sports, Science, and Technology (MEXT) of Japan, the Japan Society for the Promotion of Science (JSPS), and the Tau-Lepton Physics Research Center of Nagoya University; the Australian Research Council and the Australian Department of Industry, Innovation, Science and Research; the National Natural Science Foundation of China under contract No. 10575109, 10775142, 10875115 and 10825524; the Department of Science and Technology of India; the BK21 and WCU program of the Ministry Education Science and Technology, the CHEP SRC program and Basic Research program (grant No. R01-2008-000-10477-0) of the Korea Science and Engineering Foundation, Korea Research Foundation (KRF-2008-313-C00177), and the Korea Institute of Science and Technology Information; the Polish Ministry of Science and Higher Education; the Ministry of Education and Science of the Russian Federation and the Russian Federal Agency for Atomic Energy; the Slovenian Research Agency; the Swiss National Science Foundation; the National Science Council and the Ministry of Education of Taiwan; and the U.S. Department of Energy. This work is supported by a Grant-in-Aid from MEXT for Science Research in a Priority Area (“New Development of Flavor Physics”), and from JSPS for Creative Scientific Research (“Evolution of Tau-lepton Physics”). Author N.J.J. thanks Prof. Kazuo Abe of IPMU for illuminating discussions and guidance during the initial development of this work.

-
- [1] N. Cabibbo, Phys. Rev. Lett. **10**, 531 (1963); M. Kobayashi and T. Maskawa, Prog. Theor. Phys. **49**, 652 (1973).
- [2] I. Dunietz and R. G. Sachs, Phys. Rev. D **37**, 3186 (1988). *Erratum*: Phys. Rev. D **39**, 3515 (1989); I. Dunietz, Phys. Lett. B **427**, 179 (1998); D. A. Suprun, C.-W. Chiang and J. L. Rosner, Phys. Rev. D **65**, 054025 (2002).
- [3] M. Iwabuchi *et al.* (Belle Collab.), Phys. Rev. Lett. **101**, 041601 (2008).
- [4] C. S. Kim *et al.*, Phys. Rev. D **63**, 094506 (2001).
- [5] B. Blok, M. Gronau and J. L. Rosner, Phys. Rev. Lett. **78**, 3999 (1997).
- [6] M. Gronau and J. L. Rosner, Phys. Lett. B **666**, 185 (2008).
- [7] P. Krokovny *et al.* (Belle Collab.), Phys. Rev. Lett. **89**, 231804 (2002).
- [8] B. Aubert *et al.* (BaBar Collab.), Phys. Rev. Lett. **90**, 181803 (2003).
- [9] B. Aubert *et al.* (BaBar Collab.), Phys. Rev. Lett. **98**, 081801 (2007).
- [10] B. Aubert *et al.* (BaBar Collab.), Phys. Rev. D **78**, 032005 (2008).
- [11] Inclusion of the charge-conjugate states is implicit throughout this work unless otherwise stated.
- [12] S. Kurokawa and E. Kikutani, Nucl. Instrum. Meth. A **499**, 1 (2003), and other papers included in this volume.
- [13] A. Abashian *et al.* (Belle Collab.), Nucl. Instrum. Meth. A **479**, 117 (2002).
- [14] Z. Natkaniec *et al.* (Belle SVD2 Group), Nucl. Instrum. Meth. A **560**, 1 (2006).
- [15] C. Amsler *et al.* (Particle Data Group), Phys. Lett. B **667**, 1 (2008).
- [16] K.-F. Chen *et al.* (Belle Collab.), Phys. Rev. D **72**, 012004 (2005).
- [17] The Fox-Wolfram moments were introduced in G. C. Fox and S. Wolfram, Phys. Rev. Lett. **41**, 1581 (1978). The Fisher discriminant used by Belle, based on modified Fox-Wolfram moments (SFW), is described in K. Abe *et al.* (Belle Collab.), Phys. Rev. Lett. **87**, 101801 (2001) and K. Abe *et al.* (Belle Collab.), Phys. Lett. B **511**, 151 (2001).
- [18] S. H. Lee *et al.* (Belle Collab.), Phys. Rev. Lett. **91**, 261801 (2003).
- [19] For MC event generation, EvtGen, described in D. J. Lange, Nucl. Instrum. Meth. A **462**, 152 (2001) is used, while the detector performance is simulated using GEANT, described in R. Brun *et al.*, CERN-DD-78-2-Rev, CERN-DD-78-2, Jul 1978.
- [20] J. E. Gaiser *et al.* (Crystal Ball Collab.), Phys. Rev. D **34**, 711 (1986).
- [21] E. Follana *et al.*, Phys. Rev. Lett. **100**, 062002 (2008).
- [22] D. Becirevic *et al.*, hep-lat/0011075 and the references therein.
- [23] M. Neubert, Phys. Rept. **245**, 259 (1994).